ELSEVIER

Biochimica et Biophysica Acta 1464 (2000) 104–112

BIOCHIMICA ET BIOPHYSICA ACTA
BBA

www.elsevier.com/locate/bba

Solution conformations of short-chain phosphatidylcholine Substrates of the phosphatidylcholine-preferring PLC of *Bacillus cereus*

Stephen F. Martin *, Gregory E. Pitzer

Department of Chemistry and Biochemistry, University of Texas, Austin, TX 78712, USA

Received 30 August 1999; received in revised form 2 December 1999; accepted 13 December 1999

Abstract

The phosphatidylcholine (PC)-preferring phospholipase C (PLC) from *Bacillus cereus* (PLC_{Bc}) hydrolyzes various 1,2-diacyl derivatives of PC at different rates. Substrates with side chains having eight or more carbons are present in micellular form in aqueous media and are processed most rapidly. The catalytic efficiency (k_{cat}/K_m) for the hydrolyses of short-chain PCs at concentrations below their respective critical micelle concentrations also decreases as the side chains become shorter, and this loss of efficiency owes its origin to increases in K_m. In order to ascertain whether the observed increases in K_m might arise from conformational changes in the glycerol backbone, nuclear magnetic resonance (NMR) experiments were performed in D_2O to determine the $^3J_{HH}$ and $^3J_{CH}$ coupling constants along the glycerol subunit of 1,2-dipropanoyl-*sn*-glycero-3-phosphocholine ($K_m = 61$ mM), 1,2-dibutanoyl-*sn*-glycero-3-phosphocholine ($K_m = 21.2$ mM) and 1,2-dihexanoyl-*sn*-glycero-3-phosphocholine ($K_m = 2.4$ mM). Using these coupling constants, the fractional populations for each rotamer about the backbone of each of substrate were calculated. Two rotamers, which were approximately equally populated, about the *sn*-1–*sn*-2 bond of each substrate were significantly preferred, and in these conformers, the oxygens on the *sn*-1 and *sn*-2 carbons of the backbone were synclinal to optimize intramolecular hydrophobic interactions between the acyl side chains. There was greater flexibility about the *sn*-2–*sn*-3 bond, and each of the three possible staggered conformations was significantly populated, although there was a slight preference for the rotamer in which the oxygen bearing the phosphate head group was synclinal to the oxygen at the *sn*-2 carbon and to the *sn*-1 carbon; in this orientation, the head group is folded back relative to the side chains. These studies demonstrate that there is no significant change in the conformation about the glycerol backbone as a function of side chain length in short-chain phospholipids. Thus, prior organization of the substrate seems an unlikely determinant of the catalytic efficiency of PLC_{Bc}, and other factors such as hydrophobic interactions or differential solvation/desolvation effects associated with the complexation of the substrate with PLC_{Bc} may be involved.

Keywords: Phosphatidylcholine; Phospholipid conformation; Glycerol backbone; Nuclear magnetic resonance

Abbreviations: PLC, phospholipase C; PLC_{Bc}, phosphatidylcholine-preferring phospholipase C from *Bacillus cereus*; C6PC, 1,2-dihexanoyl-*sn*-glycero-3-phosphocholine; C4PC, 1,2-dibutanoyl-*sn*-glycero-3-phosphocholine; C3PC, 1,2-dipropanoyl-*sn*-glycero-3-phosphocholine; CMC, critical micelle concentration; PAN, 1-(2-pyridylazo)-2-naphthol; NMR, nuclear magnetic resonance; HETLOC, heteronuclear long range coupling

* Corresponding author. Fax: +1 (512) 471-4180; E-mail: sfmartin@mail.utexas.edu

0005-2736/00/$ – see front matter
PII: S0005-2736(99)00252-7

1. Introduction

Phospholipids are the fundamental components of biological membranes, and hence knowledge of the structure, function and mechanism of the various enzymes that are involved in phospholipid synthesis and hydrolysis is important. Of the enzymes that process phospholipids, members of the phospholipase C (PLC) class, which catalyze the hydrolysis of the phospholipid into diacylglycerol (DAG) and a phosphorylated head group, have received extensive attention owing to their involvement in cellular signal transduction in mammalian systems [1]. For example, DAG is a second messenger in these signaling cascades. The phosphatidylcholine (PC)-preferring PLC from *Bacillus cereus* (PLC_{Bc}) (EC 3.1.4.3) is a member of this class of enzymes that has three zinc ions at its active site [2]. Because of its unusual trimetal center coupled with its antigenic similarity to a mammalian PLC [3], PLC_{Bc} has been the subject of numerous investigations to elucidate its structure, function and mechanism [4–10].

The efficiency with which PLC_{Bc} hydrolyzes PCs having different lengths of acyl side chains has been examined as a step toward establishing the essential features of substrate structure-activity relationships. These studies revealed that micellar substrates, which typically have side chains that each contain eight or more carbons, were hydrolyzed significantly faster than soluble ones; there was also a marked discontinuity in the rate curves at the critical micelle concentration (CMC) for a given substrate [11–14]. Because the interpretation of kinetic data obtained in heterogeneous systems can be problematic, mechanistic and kinetic studies are best performed with water-soluble PC derivatives, even though these may not be naturally occurring. Short-chain PCs with either six or seven carbons in each side chain exhibited comparable K_ms (i.e. 0.36 and 0.20 mM, respectively) and V_{max}s (1000 and 1340 μM/min/mg, respectively) in solution, whereas the corresponding lecithin with fur carbons in each chain was a much poorer substrate ($K_m = 40$ mM, $V_{max} = 750$ μM/min/mg) [12]. Thus, reducing the length of acyl side chains on soluble substrates results in a significant decrease in the catalytic efficiency of PLC_{Bc}, and the major effect is to increase K_m. Inasmuch as preorganization of the substrate could have an effect upon the observed

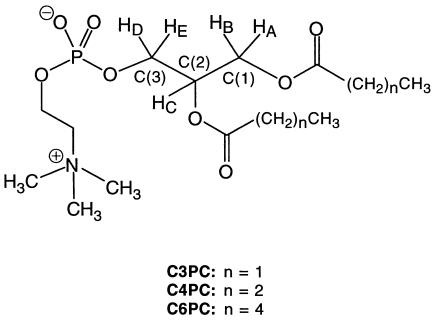

Fig. 1. A schematic drawing of PC with stereochemical numbering and hydrogen labels adapted from Hauser [21]. For C3PC, $n = 1$; C4PC, $n = 2$; C6PC, $n = 4$.

K_ms, we undertook a nuclear magnetic resonance (NMR) study to compare the preferred structures in aqueous solutions of a series of short-chain PCs to ascertain whether there was any correlation between the solution structure of the substrate and the catalytic efficiency with which it was hydrolyzed by PLC_{Bc}.

2. Materials and methods

2.1. Materials

The short-chain phospholipids 1,2-dihexanoyl-*sn*-glycero-3-phosphocholine (C6PC), 1,2-dibutanoyl-*sn*-glycero-3-phosphocholine (C4PC) and 1,2-dipropanoyl-*sn*-glycero-3-phosphocholine (C3PC) (Fig. 1) were obtained in powder form (99% purity) from Avanti Polar Lipids (Alabaster, AL, USA). 1-(2-Pyridylazo)-2-naphthol (PAN) dye was obtained from Aldrich (Milwaukee, WI, USA). PLC_{Bc} and alkaline phosphatase were obtained from Sigma (St. Louis, MO, USA).

2.2. NMR experiments

The phospholipids were dissolved in 99% D_2O below their respective CMCs. The concentrations used were as follows: C3PC, 150 mM; C4PC, 75 mM and C6PC, 8 mM. The NMR experiments were performed on a Varian 500 MHz NMR with a triple resonance probe using the residual water peak at δ 4.63 as the reference. The proton spectra were acquired with 64K points and a resolution of 0.10 Hz/point. The heteronuclear long range coupling (HET-

LOC) experiments used the pulse sequence from Kessler [15]. The C3PC and C4PC spectra were acquired with 64 blocks of 448 increments, and the C6PC spectrum was taken with 102 blocks of 448 increments. Digital resolution for all HETLOC experiments was 0.41 Hz/point. The spectra were zero-filled to 16K points for processing.

2.3. Determination of CMC

The CMCs of C3PC and C4PC were determined in 96-well microtiter plates using a method based upon the solubilization of the dye PAN [16,17]. Briefly, the concentrations of C3PC and C4PC were made up to a final volume of 50 μl in each well of a 96-well microtiter plate. The concentrations used for C3PC were varied from 80 to 475 mM; concentrations for C4PC were varied from 20 to 780 mM. In the 96-well microtiter plate, 5 μl of 1.6 mM PAN solution in pentane was added to each phospholipid concentration. After 20 min, the pentane had evaporated and the color was fully developed; the absorbancy was then read at 470 nm. These absorbancies were graphed versus phospholipid concentration, and the CMC was determined from the intersection of the two lines according to the protocol of Furton [16].

2.4. Kinetic assays of short-chain phospholipids

Assays were performed in a 96-well format with PLC_{Bc} using a coupled chromogenic assay in which the phosphorylcholine product from the PLC_{Bc}-catalyzed hydrolysis of the soluble phospholipid is first hydrolyzed by alkaline phosphatase to liberate inorganic phosphate [8]. To quantitate the inorganic phosphate, a solution containing ammonium molybdate and ascorbic acid in trichloroacetic acid is added, followed by a second solution of sodium metaarsenite and trisodium citrate in acetic acid. The development of the blue color from the resulting molybdenum-phosphate complex is complete after 20 min, and the microplate is read at 700 nm. The assays were performed at least three times each on separate days. The kinetic parameters were determined from a non-linear least-squares fit of the data by Kaleidagraph utilizing the equation, $v = V_{max}[S]/K_m + [S]$.

3. Results

The CMCs of the short-chain PCs increase dramatically as the length of the side chains is reduced because the hydrophobic forces that drive micelle formation decrease. Using the PAN dye inclusion assay, the CMCs of C6PC, C4PC and C3PC were determined to be 8.1, 180 and 405 mM, respectively (Table 1). These values are in reasonable agreement with the corresponding values of 11.1 and >150 mM obtained independently for C6PC and C4PC [12,18]. As expected, the catalytic efficiencies of PLC_{Bc} toward the soluble substrates C6PC, C4PC and C3PC decreased as the side chains were shortened, and the primary effect was in the measured K_ms (Table 1); the k_{cat} remained relatively constant for all three substrates. The K_m for C6PC was 2.4 mM, but when the side chains are shortened to four carbon atoms, the K_m increased to 21.2 mM and to 61.0 mM for C3PC. The kinetic parameters determined in this study for C6PC and C4PC were in good qualitative agreement with those obtained in an earlier investigation in which an assay based upon a pH stat titration was used [12].

The NMR studies to probe the preferred conformations about the glycerol backbone in C6PC, C4PC and C3PC in aqueous solution were conducted in a

Table 1
Measured CMC values and kinetic parameters for the PLC_{Bc}-catalyzed hydrolysis of short-chain PCs

Substrate	CMC (mM)	V_{max} (μmol/min/mg)[a]	k_{cat} (s^{-1})[b]	K_m (mM)	K_{cat}/K_m (s/mM)
C3PC	405	2290	1090	61.0	18
C4PC	180	1430	680	21.2	32
C6PC[c]	8.1	2100	1000	2.4	417

[a]Error in V_{max}: ±250 μmol/min/mg for C3PC and ±107 μmol/min/mg for C4PC.
[b]Error in K_m: ±14.4 mM for C3PC and ±4.1 for C4PC.
[c]Data shown for C6PC have previously been reported [8,17].

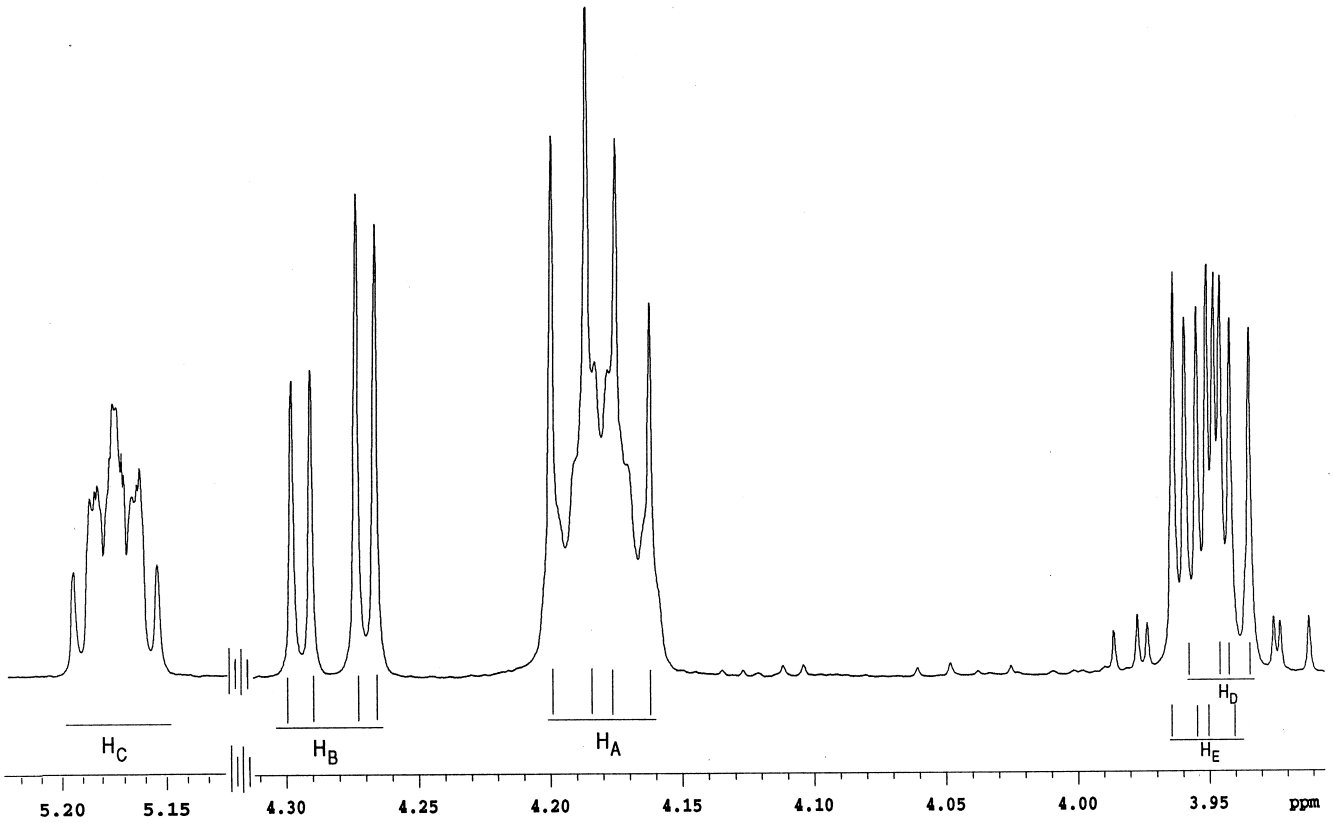

Fig. 2. Expanded portion of the proton spectrum of C3PC showing the vicinal couplings between H_A, H_B and H_C, and between H_D and H_E and H_C.

manner similar to those reported by Hauser [19,20]. The experiments were all performed in D_2O to correspond to the usual assay conditions. Moreover, the measurements were obtained at concentrations below the CMC of the PC to ensure that any packing of the side chains was due to hydrophobic forces and not to any intermolecular interactions or packing in a micelle structure. The ^1H NMR spectrum of C3PC, which is typical of the one-dimensional spectra obtained for C6PC and C4PC, is shown in Fig. 2. The assigned values for the chemical shifts and the observed vicinal coupling constants are summarized in Tables 2 and 3, respectively, for the protons on the glycerol backbones of C6PC, C4PC and C3PC (Fig. 1).

Assuming that the three staggered conformations about the C(1)–C(2) bond (rotamers A–C) and the C(2)–C(3) bond (rotamers D–F) represent rapidly interconverting, minimum energy conformations (Fig. 3), it is possible to calculate the percentage of each conformer at equilibrium using the vicinal spin-spin coupling constants. The coupling constant that is determined experimentally represents an average value that is derived from the component, three-bond coupling constants, which are associated with each of the three conformations, weighted by the

Table 2
Chemical shifts (δ) for protons on the glycerol backbone of short-chain PCs

Substrate	H_A	H_B	H_C	H_D	H_E
C3PC	4.18	4.28	5.18	3.95	3.96
C4PC	4.18	4.30	5.20	3.94	3.95
C6PC	4.17	4.31	5.18	3.94	3.95

Table 3
Measured vicinal coupling constants (Hz) of the glycerol backbone of short-chain PCs

Substrate	$^3J_{AC}$	$^3J_{BC}$	$^3J_{CD}$	$^3J_{CE}$	$^3J_{C(3)-HA}$	$^3J_{C(3)-HB}$
C3PC	6.6	3.5	4.5	5.6	2.4	2.0
C4PC	6.7	3.4	4.4	5.7	2.0	2.8
C6PC	7.0	3.2	4.5	5.6	1.2	2.0

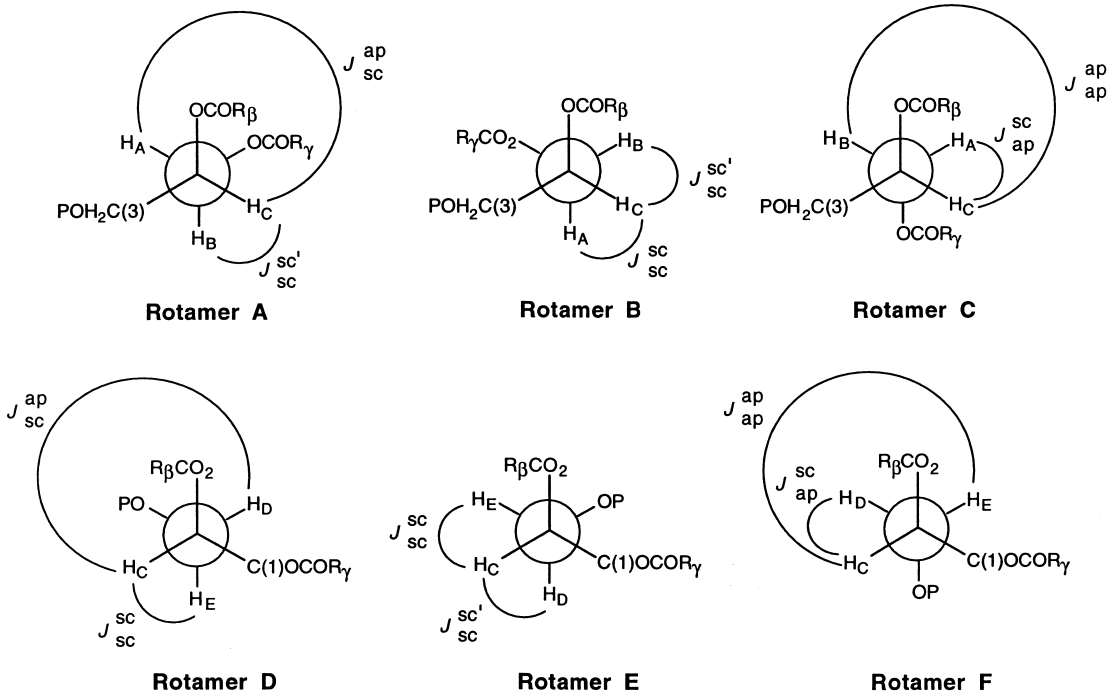

Fig. 3. Newman projections of the staggered conformation, which presumably correspond to the three low energy conformers, for PC. Component vicinal coupling constants (Hz) for rotamers A–F: $J^{ap}_{sc} = 12.3$, $J^{sc'}_{sc} = 2.4$, $J^{sc}_{sc} = 0.45$, $J^{sc}_{ap} = 5.8$ and $J^{ap}_{ap} = 11.9$. The nomenclature for the labeled coupling constant using J^{ap}_{sc} as an example is as follows: the superscript, ap (antiperiplanar), refers to the relationship between the two coupled hydrogens, whereas the subscript, sc (synclinal), refers to the orientation of the glycerol oxygens relative to each other.

fractional population of that conformer [21]. The values of the component coupling constants were taken from the literature [22,23]. The percentage of each rotamer in the two conformational families A–C and D–F for each C6PC, C4PC and C3PC were then calculated, and the results are summarized in Table 4.

Table 4
Fractional conformer populations for the C(1)–C(2) (rotamers A–C) and C(2)–C(3) (rotamers D–F) bonds of the glycerol backbone of short-chain PCs

Substrate	A	B	C	D	E	F
C3PC	46	41	12	19 (33)	47 (45)	34 (22)
C4PC	48	41	11	18 (35)	47 (44)	35 (21)
C6PC	51	41	8	19 (34)	47 (44)	34 (22)

For the torsion angles defining conformers A–C, the rotamer composition is based on the assumption that $^3J_{AC} > {}^3J_{BC}$. If $^3J_{BC} > {}^3J_{AC}$, rotamer C, in which the acyl side chains would be antiperiplanar thus not allowing the well-known parallel packing, would become significantly populated. For rotamers D–F, two sets of values are obtained for each rotamer depending upon whether $^3J_{CE} > {}^3J_{CD}$ or $^3J_{CD} > {}^3J_{CE}$ (in parentheses).

Correlating three-bond heteronuclear coupling constants with Karplus-like curves may also provide information regarding dihedral angles [24]. For example, information regarding the average dihedral angle about the C(1)–C(2) bond may be obtained from $^3J_{C(3)-HA}$ and $^3J_{C(3)-HB}$, whereas the average dihedral angle about the C(2)–C(3) bond is derived from $^3J_{C(1)-HD}$ and $^3J_{C(1)-HE}$. These heteronuclear coupling constants may be determined using a two-dimensional HETLOC NMR experiment that provides total correlation spectra in which the signal for a proton is split into a doublet in each of the two frequency domains by a ^{13}C atom giving an E.COSY-like pattern. A region of such a spectrum corresponding to H_A and H_B of C3PC is shown in Fig. 4. The doublets observed for H_A and H_B in the F1 domain correspond to the heteronuclear one-bond couplings $^1J_{C(1)-HA}$ and $^1J_{C(1)-HB}$, and the doublets for H_A and H_B in the F2 domain result from the heteronuclear three-bond couplings $^3J_{C(3)-HA}$ and $^3J_{C(3)-HB}$. The value for $^3J_{C(3)-HA}$ is then determined by selecting a slice in the F1 domain

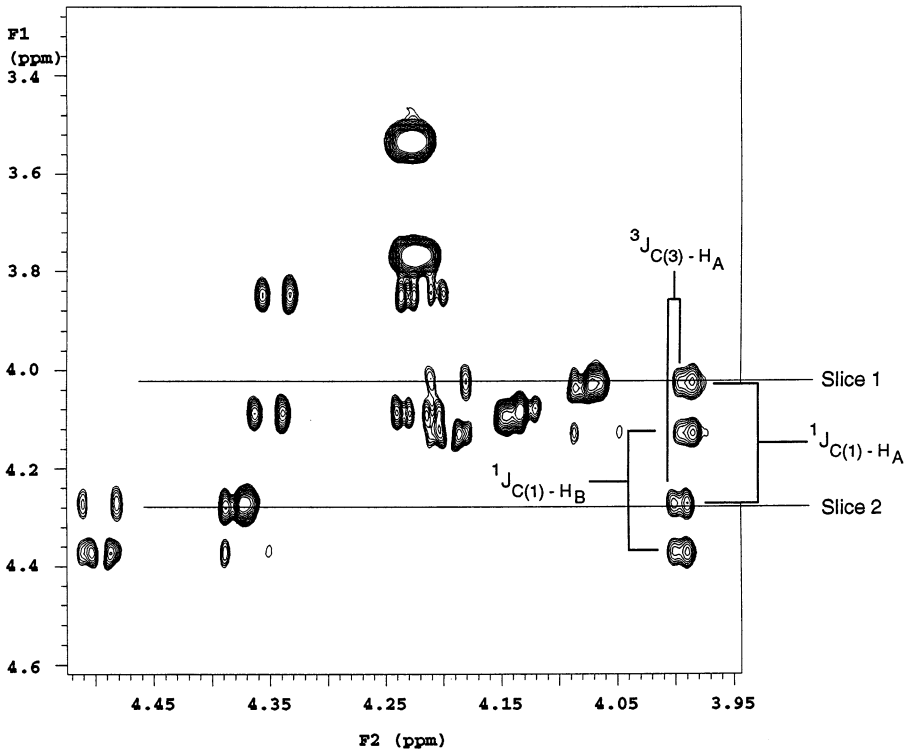

Fig. 4. HETLOC spectrum of C3PC showing the doublets resulting from coupling between C(3) and the hydrogens H_A and H_B on C(1).

for each peak associated with H_A and measuring the difference in the chemical shifts in the F2 domain for the two peaks associated with H_A (Fig. 5). The value of $^3J_{C(3)-HB}$ was determined analogously. The values thus obtained for $^3J_{C(3)-HA}$ and $^3J_{C(3)-HB}$ for C3PC were 2.4 and 2.0 Hz, respectively (Table 3); similar values were obtained for C4PC and C6PC (Table 3). However, because the signal-to-noise ratio in the later spectrum was high, the values for the two heteronuclear coupling constants are somewhat less reliable. Owing to the overlap of peaks for H_D and H_E, it was not possible to determine the coupling constants $^3J_{C(1)-HD}$ and $^3J_{C(1)-HE}$ using the HETLOC experiment.

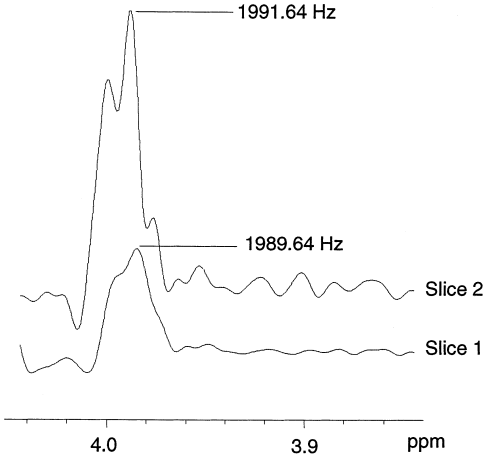

Fig. 5. Slices extracted from the HETLOC NMR spectrum for H(A) of C3PC. The magnitude of the coupling constant is calculated from the difference in the chemical shifts of the peaks.

4. Discussion

The catalytic efficiency with which PLC_{Bc} hydrolyzes PC derivatives depends upon the length of the acyl side chains. Micellar substrates are hydrolyzed faster than monomolecular dissolved ones, and there is a marked discontinuity at the CMC at which a 3-fold increase is typically observed in the V_{max}. For PCs containing six or seven carbon atoms in each side chain, the apparent K_m for the soluble form is about 10 times higher than for the micellar form [11,12]. In the present work, we determined the kinetic parameters for the water-soluble PCs C6PC,

C4PC and C3PC. Although there was little variation in the measured k_{cat}s, there was a 10–25-fold increase in the observed K_ms as the acyl side chains were shortened (Table 1). There is therefore a significant decrease in the efficiency of the PLC_{Bc}-catalyzed hydrolysis of soluble PCs as the length of the side chains is decreased, and this loss of efficiency is manifested primarily in increases in K_m. The objective of the present study was to probe the basis for this difference in enzymatic efficiency by examining whether the preferred backbone conformations of soluble PCs varied as a function of side chain length.

Because PC is the most abundant phospholipid in cellular and subcellular membranes, X-ray crystallography [25,26] and NMR [19,20,27–32] have been extensively utilized to determine the preferred conformation(s) of various PCs in different environments. In organized environments such as those imposed in micelles and liquid crystals, PCs adopt three-dimensional structures that are reasonably well-defined. There is a clear preference about the C(1)–C(2) bond for rotamers A and B in which the hydrophobic acyl side chains pack in parallel conformations, but there is somewhat greater flexibility about the C(2)–C(3) bond with rotamers D–F being more equally populated (Fig. 4). In solution, however, the molecules are not constrained by intermolecular packing forces, and there is potentially greater freedom for rotations about the glycerol backbone that would alter the relative orientations of the acyl side chains and the phosphate moiety of the head group. This increased flexibility in solution might lead to preferred structures different from those found in micelles and bilayers. Nevertheless, the parallel packing of the side chains clearly plays a major role in determining conformational preferences about the C(1)–C(2) bond of PCs both in solution and in micelles. However, it was not known whether PCs containing six or fewer carbon atoms in each side chain adopt the same preferred conformations. To address this important question, we performed a series of NMR experiments in D_2O to establish the conformational preferences about the glycerol backbone of the soluble PCs C6PC, C4PC and C3PC.

The vicinal coupling constants for the protons on the glycerol backbones of C6PC, C4PC and C3PC were determined by ^1H NMR spectroscopy (Table 3), and these average values were used to calculate the fractional populations of the three staggered conformations about each of the C(1)–C(2) and C(2)–C(3) bonds (Table 4). The conformational preferences are most easily derived from analysis of the vicinal couplings between the backbone protons. The data obtained from the heteronuclear, three-bond coupling constants $^3J_{C(3)-HA}$ and $^3J_{C(3)-HB}$ are also useful, but the experimentally determined values of these coupling constants represent an average derived from the fractional populations of the different rotamers A–C and the component, heteronuclear coupling constants, which unfortunately are unknown. Nevertheless, based upon the operative Karplus relationship, the expected heteronuclear coupling constant $^3J_{CH}$ is 2.0 Hz for a dihedral angle of (±) 60° and 8.8 Hz for 180° [24]. Thus, the observed coupling constants $^3J_{C(3)-HA}$ and $^3J_{C(3)-HB}$ for each of the short-chain PCs are consistent with preferred conformations in which there is an approximate (±) 60° relationship between C(3) and both H_A and H_B.

The relative percentages of each rotamer for the short-chain PCs C6PC, C4PC and C3PC reveal that there is little difference in the preferred solution conformation about the glycerol backbone as a function of side chain length. Thus, even though the intramolecular hydrophobic interactions were expected to decrease significantly in reducing the acyl side chain length from six to three carbons, any such decrease was not manifested in observable conformational changes. In each case, the dominant conformations about the C(1)–C(2) bond were A and B, which allow for hydrophobic interactions between the chains. There was a slight increase ($< 5\%$) in the population of rotamer C for C4PC and C3PC relative to C6PC, but this change seems unlikely to account for the more dramatic 10–25-fold difference observed in the catalytic efficiencies for these substrates. Although there is a slight preference for rotamer E, there is little difference in the relative energies of the three possible staggered conformations about the C(2)–C(3) bond for C6PC, C4PC and C3PC, suggesting that the length of the fatty acid side chain does not significantly effect the orientation of the head group relative to the backbone. These findings are in good agreement with the literature data for the conformational preferences of C6PC in aqueous solution [19,20]. In this context, it is perhaps interesting to note that dominant conformer about the C(2)–C(3)

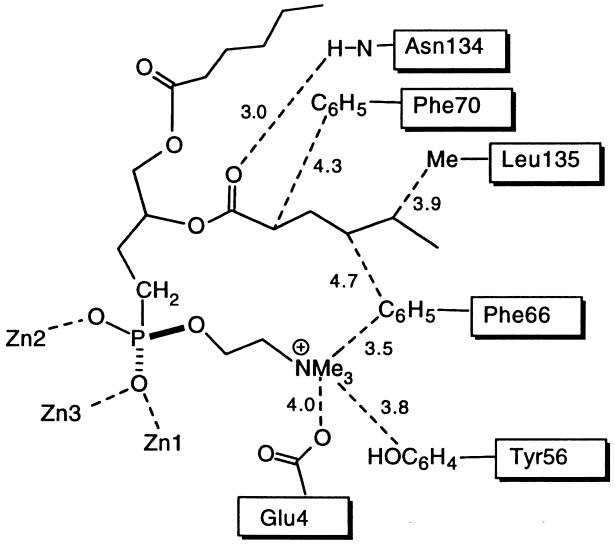

Fig. 6. Possible interactions between the side chains of PLC_{Bc} and the backbone of a phosphonate inhibitor. All distances are in Å. Adapted from [5].

bond of 1,2-*O*-dimyristoyl-*sn*-glycero-3-phosphocholine in the liquid crystalline phase is rotamer D [30].

Decreases in the hydrophobic interactions arising from shorter side chains thus do not appear to influence significantly the orientations of substituents on the glycerol backbone of the soluble PCs in this study. Prior organization of the substrate in a conformation that interacts optimally with the enzyme active site then seems an unlikely explanation for the observed decrease in the catalytic efficiency of PLC_{Bc} toward soluble substrates. It should be noted, however, that these experiments explored only whether side chain length effected the conformation of the glycerol backbone and not whether there were changes in how the side chains packed. Such effects could be explored by nOe (NOESY) studies, but because of the magnetic equivalence of protons on the two side chains in the unlabeled PCs, it was not possible to distinguish unambiguously intrachain interactions from interchain interactions.

Thus, the question is now: if an internal hydrophobic effect is not involved, what is responsible for the large increase in K_m that is observed in the PLC_{Bc}-catalyzed hydrolysis of soluble PCs having acyl side chains of decreasing lengths? Examination of the crystal structure of PLC_{Bc} complexed with the phosphonate inhibitor 3(*S*),4-dihexanoyloxybutyl-1-phosphonylcholine, which has six carbons in the side chains, reveals that the ammonium ion of the choline moiety lies in a pocket formed by Glu-4, Tyr-56 and Phe-66 (Fig. 6) [5]. In this structure, the conformations about the C(1)–C(2) and C(2)–C(3) bonds of the bound inhibitor correspond to rotamers B and F. The only close contact observed between an acyl side chain on the substrate and the enzyme in this structure was between the methyl groups of Leu-135 and C(5) of the *sn*-2 side chain, and this distance was approximately 3.9 Å; another possible contact (4.5 Å) is with C(6) on the side chain.

Because there did not appear to be more extensive interactions between the inhibitor and PLC_{Bc}, we originally discounted the possibility that hydrophobic interactions between the acyl side chains of a substrate and residues on the enzyme would contribute significantly to binding and catalytic efficiency. On closer inspection of the X-ray data of this complex, however, it may be seen that there is considerable thermal motion associated with the acyl side chains, especially the *sn*-1 chain, and so it is quite possible that the side chains of Phe-66, which is about 4.4 Å from C(4) of the *sn*-2 chain, and perhaps Phe-70, which is about 4.2 Å from C(2) of the *sn*-2 side chain, could be involved in binding the acyl side chains of either the substrate or the product DAG. In the absence of these favorable interactions, K_m could increase. Thus, the combined hydrophobic interactions between Leu-135, Phe-66 and Phe-70 and a substrate (or inhibitor) could play an important role in recognition and/or binding. Moreover, it is necessary to carefully examine and evaluate the solvation/desolvation effects associated with the complexation of different soluble PC substrates with PLC_{Bc}. The basis of the observed hydrophobic effect upon catalytic efficiency of PLC_{Bc} is presently the subject of a series of studies, the results of which will be reported in due course.

Acknowledgements

We thank the National Institutes of Health and the Robert A. Welch Foundation for their generous support of this research. We also thank Steve Sorey (University of Texas at Austin) for his assistance in implementing the HETLOC pulse sequence.

References

[1] J.C. Exton, Eur. J. Biochem. 243 (1997) 10–20.
[2] E. Hough, L.K. Hansen, B. Birkness, K. Jynge, S. Hansen, A. Hordvik, C. Little, E. Dodson, Z. Derewenda, Nature 338 (1989) 357–360.
[3] M.A. Clark, R.G.L. Shorr, J.S. Bomalaski, Biochem. Biophys. Res. Commun. 140 (1986) 114–119.
[4] M.F. Roberts, in: E.A. Dennis (Ed.), Methods in Enzymology, Academic Press, San Diego, CA, 1991, pp. 95–112.
[5] S. Hansen, E. Hough, L.A. Svensson, Y.-L. Wong, S.F. Martin, J. Mol. Biol. 234 (1993) 179–187.
[6] E. Hough and S. Hansen, in: P. Woolley and S.B. Petersen (Eds.), Lipases. Their Structure, Biochemistry and Application, University Press, Cambridge, 1994, pp. 95–118.
[7] S.F. Martin, M.R. Spaller, P.J. Hergenrother, Biochemistry 35 (1996) 12970–12977.
[8] P.J. Hergenrother, S.F. Martin, Anal. Biochem. 251 (1997) 45–49.
[9] S.F. Martin, P.J. Hergenrother, Biochemistry 37 (1998) 5755–5760.
[10] S.F. Martin, P.J. Hergenrother, Biochemistry 38 (1999) 4403–4408.
[11] C. Little, Acta Chem. Scand. B31 (1977) 267–272.
[12] M. El-Sayed, C. DeBose, L. Coury, M. Roberts, Biochim. Biophys. Acta 837 (1985) 325–335.
[13] N.E. Gabriel, N.V. Agman, M.F. Roberts, Biochemistry 26 (1987) 7409–7418.
[14] K. Lewis, J. Bian, A. Sweeney, M. Roberts, Biochemistry 29 (1990) 9962–9970.
[15] M. Kurz, P. Schmieder, H. Kessler, Angew. Chem. Int. Ed. Engl. 30 (1991) 1329–1331.
[16] K.G. Furton, A. Norelus, J. Chem. Ed. 70 (1993) 254–257.
[17] P.J. Hergenrother, M.K. Hass, S.F. Martin, Lipids 32 (1997) 783–788.
[18] D. Geng, D. Baker, S. Foley, C. Zhou, K. Stieglitz, M. Roberts, Biochim. Biophys. Acta 1430 (1999) 234–244.
[19] H. Hauser, W. Guyer, I. Pascher, P. Skrabal, S. Sundell, Biochemistry 19 (1980) 366–373.
[20] H. Hauser, I. Pascher, S. Sundell, Biochemistry 27 (1988) 9166–9174.
[21] H. Hauser, W. Guyer, B. Levine, P. Skrabal, R.J.P. Williams, Biochim. Biophys. Acta 508 (1978) 450–463.
[22] R.J. Abraham and G. Gatti, J. Chem. Soc. (B) (1969), 961–968.
[23] G. Gatti, A. Segre, C. Morandi, Tetrahedron 23 (1967) 4385–4393.
[24] J.L. Marshall, Carbon-Carbon and Carbon-Proton NMR Couplings: Applications to Organic Stereochemistry and Conformational Analysis, Verlag Chemie International, Deerfield Beach, FL, 1983.
[25] I. Pascher, M. Lundmark, P. Nyholm, S. Sundell, Biochim. Biophys. Acta 1113 (1992) 339–373.
[26] H. Hauser, I. Pascher, R. Pearson, S. Sundell, Biochim. Biophys. Acta 650 (1981) 21–51.
[27] J.R.A. Burns, M.F. Roberts, Biochemistry 19 (1980) 3100–3106.
[28] S. Smith, I. Kustanovich, S. Bhamidipati, A. Salmon, J. Hamilton, Biochemistry 31 (1992) 11660–11664.
[29] M. Hong, K. Schimdt-Rohr, D. Nanz, Biophys. J. 69 (1995) 1939–1950.
[30] M. Hong, K. Schmidt-Rohr, H. Zimmerman, Biochemistry 35 (1996) 8335–8341.
[31] A. Arora, C. Gupta, Biochim. Biophys. Acta 1324 (1997) 47–60.
[32] K. Bruzik, J. Harwood, J. Am. Chem. Soc. 119 (1997) 6629–6637.